Particle Coarsening II: Growth Kinetics of Hydrothermal $BaTiO_3$

Weian Sun,*,† Yan Pang,‡ Junqin Li,† and Weiqin Ao†

College of Material Science and Engineering, Shenzhen University, Shenzhen Key Laboratory of Special Functional Materials, Shenzhen 518060, China, and College of Chemistry and Chemical Engineering, Shenzhen University, Shenzhen 518060, China

Received July 25, 2006. Revised Manuscript Received February 2, 2007

Coarsening of barium titanate ($BaTiO_3$) particles under hydrothermal conditions was investigated theoretically and experimentally. A detailed model, in which coarsening is assumed to be controlled by a reversible interface reaction, is presented and discussed. The model predicts a linear growth law $R - R_0 = Kt$ in the early stage of coarsening. This result is supported by the experimental data collected for conventional and microwave-assisted hydrothermal syntheses at two different temperatures. The growth constant K corresponds to a nonlinear combination of thermodynamic and kinetic parameters. Under microwave irradiation, the growth rate was found to be 1 order of magnitude larger than in a conventional hydrothermal process. The predicted variation of the growth kinetics, from linear to parabolic, was observed experimentally at long reaction times.

I. Introduction

Barium titanate is widely used in the electronics industry as a primary material because of its excellent ferroelectric and dielectric properties. The rapid development in multilayered ceramic capacitors (MLCCs) requires fine and uniform $BaTiO_3$ powders.[1−2] The application of nanostructured $BaTiO_3$ in ferroelectric nonvolatile memory promises to increase memory density thousands fold by reading and writing into individual particles.[3−4] However, it has been known that the ferroelectric and dielectric properties, and hence the applications, depend on the size of $BaTiO_3$ particles.[5−9]

Among the various synthesis methods, the hydrothermal route is of considerable interest. Fine and uniform ceramic powders of high purity can be readily prepared through the hydrothermal method in a single step without requiring elaborate apparatus or expensive reagents.[10−11] Recently, an alternative microwave hydrothermal (MH) process has been developed because of its advantages in terms of rapid kinetics and enhanced energy efficiency over the conventional hydrothermal (CH) method.[12−18] Crystalline $BaTiO_3$ can be obtained within 15 min by the MH method.[13] However, to produce particles of desired size, the reaction time is always prolonged. When the supersaturation becomes very low, the growth of the crystalline $BaTiO_3$ particles should follow the coarsening or Ostwald ripening mechanism, also called as dissolution/recrystallization when solute is transferred from solution to solid phase. In the coarsening process, large particles grow at the expense of the dissolution of small particles, driven by the tendency to reduce the interface energy. In the literature, only a few studies have been reported on kinetics of coarsening of hydrothermal $BaTiO_3$,[19] though this subject is obviously of scientific and technological importance.

Theories predict that particle growth during coarsening follows a temporal power law $\bar{R}^n = Kt$.[20−26] The growth exponent n, according to LSW theory, takes value 3 or 2 depending on the coarsening being controlled by diffusion or by a interface reaction in the late stage of coarsening.[20−22] However, for some practical systems, the asymptotic coarsening state can be quite long and may be never attained in the time scale of the experiments.[27] In the previous paper, we completed an investigation into the kinetics in the early stage of coarsening controlled by a reversible interface

* Corresponding author. Tel.: 86-755-26538537. Fax: 86-755-26536239. E-mail: sunweian@21cn.com.
† College of Material Science and Engineering, Shenzhen University.
‡ College of Chemistry and Chemical Engineering, Shenzhen University.

(1) Hennings, D.; Klee, M.; Waser, R. *Adv. Mater.* **1991**, *3*, 334.
(2) Wada, S.; Yasuno, H.; Hoshina, T.; Nam, S.-M.; Kakemoto, H.; Tsurumi, T. *Jpn. J. Appl. Phys.* **2003**, *42*, 6188.
(3) Scott, J. F.; Paz de Araujo, C. A. *Science* **1989**, *246*, 1400.
(4) Yun, W. S.; Urban, J. J.; Gu, Q.; Park, H. *Nano Lett.* **2002**, *2*, 447.
(5) Begg, B. D.; Vance, E. R.; Nowotny, J. *J. Am. Ceram. Soc.* **1994**, *77*, 3186.
(6) Schlag, S.; Eicke, H. F.; Stern, W. B. *Ferroelectrics* **1995**, *173*, 351.
(7) Viswanath, R. N.; Ramasamy, S. *NanoStruct. Mater.* **1997**, *8*, 155.
(8) Lo, V. C. *J. Appl. Phys.* **2003**, *94*, 3353.
(9) Sun, W. *J. Appl. Phys.* **2006**, *100*, 083503.
(10) Dutta, P. K.; Gregg, J. R. *Chem. Mater.* **1992**, *4*, 843.
(11) Asiaie, R.; Zhug, W.; Akbar, S. A.; Dutta, P. K. *Chem. Mater.* **1996**, *8*, 226.
(12) Komarneni, S.; Roy, R.; Li, Q. H. *Mater. Res. Bull.* **1992**, *27*, 1393.
(13) Liu, S.-F.; Abothu, I. R.; Komameni, S. *Mater. Lett.* **1999**, *38*, 344.
(14) Ma, Y.; Vileno, E.; Suib, S. L.; Dutta, P. K. *Chem. Mater.* **1997**, *9*, 3023.
(15) Khollam, Y. B.; Deshpande, A. S.; Patil, A. J.; Potdar, H. S.; Deshpande, S. B.; Date, S. K. *Mater. Chem. Phys.* **2001**, *71*, 304.
(16) Sun, W.; Li, J.; Liu, W.; Li, C. *J. Am. Ceram.* Soc. **2006**, *89*, 118.
(17) Sun, W.; Li, J. *Mater. Lett.* **2006**, *60*, 1559.
(18) Sun, W.; Li, C.; Li, J.; Liu, W. *Mater. Chem. Phys.* **2006**, *97*, 481.
(19) Testino, A.; Buscaglia, V.; Buscaglia, M. T.; Viviani, M.; Nanni, P. *Chem. Mater.* **2005**, *17*, 5346.
(20) Lifshitz, I. M.; Slyozov, V. V. *J. Phys. Chem. Solids* **1961**, *19*, 35.
(21) Wagner, C. *Z. Elektrochem.* **1961**, *65*, 581.
(22) Hillert, M. *Acta Metall.* **1965**, *13*, 227.
(23) Marsh, S. P.; Glicksman, M. E. *Acta Mater.* **1996**, *44*, 3761.
(24) Baldan, A. *J. Mater. Sci.* **2002**, *37*, 2171.
(25) Ardell, A. J.; Ozolins, V. *Nat. Mater.* **2005**, *4*, 309.
(26) Gusak, A. M.; Lutsenko, G. V.; Tu, K. N. *Acta Mater.* **2006**, *54*, 785.
(27) Fan, D.; Chen, S. P.; Chen, L.-Q.; Voorhees, P. W. *Acta Mater.* **2002**, *50*, 1895.

10.1021/cm061741n CCC: $37.00
Published on Web 03/09/2007

reaction.[28] The average radius was predicted to increase linearly with time. In this work, the model with some modifications was applied to the coarsening of hydrothermal $BaTiO_3$. Experiments of MH and CH syntheses were conducted to compare with the theory.

II. Experimental Section

Reagent $Ba(OH)_2 \cdot 8H_2O$ and hydrous titanium oxide, obtained from aqueous $TiCl_4$,[16] were used as starting materials. The initial reactant composition was a Ti concentration (C_{Ti}) of 0.525 mol/dm^3 and a$Ba(OH)_2$ concentration of 1.68 mol/dm^3, which gave an initial Ba/Ti molar ratio of 3.2. Such high concentrations used here were for promoting particle growth and providing a large excess of $Ba(OH)_2$ after the formation of crystalline $BaTiO_3$.

The MH reactions were performed using a lab-made microwave-heating-autoclave system.[16−17] The system operates at the microwave frequency of 2.45 GHz and can operate at 0−100% full power of 650 W. An auxiliary cooling/heating device is fitted to the system, which enables the system to operate at a fixed temperature for a long time while maintaining the input power of the microwave radiation during the reaction. The CH processes were conducted in a stainless-steel autoclave.

The hydrous titanium oxide and $Ba(OH)_2 \cdot 8H_2O$ were put into the autoclave, followed by distilled water until a filling degree of ~70% was reached. The autoclave was heated by the conventional method in the CH process or by microwave radiation with the power kept at 550 W in the MH process. It took ~30 min to reach the desired temperature of 220 or 240 °C, at which the MH or CH synthesis was conducted for a period of time. After the reaction, the autoclave was cooled rapidly. The resulting $BaTiO_3$ powders were centrifuged and thoroughly washed. Aqueous acetic acid at a concentration of 0.1 mol/dm^3 was used to wash the products to remove the barium carbonate that was possibly in existence. The products were finally oven-dried at 90 °C for 12 h.

X-ray diffraction (XRD) analyses were performed by the Philips X'pert powder diffractometer system using Cu Kα source. The crystallite size (d_{XRD}) was estimated from the full-width at half-maximum (fwhm) of the (111) peak by Scherrer formula. A sintered sample of $BaTiO_3$ disk was used as the standard that had a very narrow fwhm of 0.086° of the (111) plane.

The particle size and morphology of the products were analyzed using scanning electron microscopy (SEM, JSM-5910). The average particle size was determined by measuring the diameters of more than 200 particles using the intercept method from the SEM images.

III. Theory

It is assumed that the coarsening of hydrothermal $BaTiO_3$ is controlled by a reversible interface reaction, in consideration of the drastic decrease in the viscosity of water under the hydrothermal conditions. From the thermodynamic data provided by Lencka and Riman,[29] the calculations indicate that in a basic solution with temperatures above 200 °C, the soluble Ti species mainly exists in the forms of $Ti(OH)_4$ and $HTiO_3^-$, and the dissolved Ba species exits as $BaOH^+$ and Ba^{2+}. Considering that the number of the reactant molecules involved in an elementary reaction seldom exceeds 2, the reversible dissolution and deposition reactions at a $BaTiO_3$ particle surface are assumed to be

$$BaTiO_3(s) + H_2O \underset{k_g}{\overset{k_d}{\rightleftharpoons}} BaOH^+ + HTiO_3^- \quad (1)$$

where k_d and k_g are the rate coefficients of dissolution and deposition, respectively. The k_d ought to depend on the activity of the particle and hence be a function of the radius R of the particle. In contrast, the k_g is independent of R, because the reactants involved are in the liquid phase.[28] For convenience, the $BaTiO_3$ particle is assumed to be chemically stoichiometric and in a spherical shape. Because the coarsening is controlled by interface reaction, the concentrations of solutes in the solution are assumed to be uniform. According to the law of mass action, the dissolution and deposition rates r_d and r_g at particle surface per unit area are

$$r_d = k_d \text{ and } r_g = k_g C_{HTiO3} C_{BaOH} \quad (2)$$

respectively. The C_{BaOH} and C_{HTiO3} are the concentrations of $BaOH^+$ and $HTiO_3^-$, respectively. The net deposition rate r_G is $r_G = r_g - r_d$. The contribution of solvent H_2O is included in k_d.

In the case in which the interface free energy should be taken into account, the chemical potential μ_R of the particle is expressed as $\mu_R = \mu_\infty + 2\gamma v_m/R$, where μ_∞ is the chemical potential of a particle of infinite size, γ is the specific interfacial free energy, and v_m is the molar volume of $BaTiO_3$. When using C^*_{HTiO3} and C^*_{BaOH} to denote the concentrations of $HT_iO_3^-$ and $BaOH^+$ in equilibrium with the given particle, and $C_{HTiO3,\infty}$ and $C_{BaOH,\infty}$ to denote the concentrations in equilibrium with a particle of infinite size, respectively, the equilibrium of reaction 1 requires

$$C^*_{HTiO3} C^*_{BaOH} = C_{HTiO3,\infty} C_{BaOH,\infty} \exp(l/R) \quad (3)$$

where the capillary length $l = 2\gamma v_m / R_A T$ with R_A denoting the universal gas constant. The equilibrium means $r_G = r_g - r_d = 0$, which, through eq 2, gives

$$k_d = k_g C^*_{HTiO3} C^*_{BaOH} \quad (4)$$

If using $k_{d,\infty}$ to represent the dissolution coefficient for bulk $BaTiO_3$, eq 2 or 4 gives

$$k_{d,\infty} = k_g C_{HTiO3,\infty} C_{BaOH,\infty} \quad (5)$$

Because coarsening originates from the particle size distribution, there must be a so-called critical size R_c: particles of radius $R < R_c$ will dissolve, whereas particles of size $R > R_c$ will grow. It implies that the particle of radius R_c is in equilibrium with the solutes $HT_iO_3^+$ and $BaOH^-$ of concentrations C_{HTiO3} and C_{BaOH}, respectively. So, according to eq 3, there is

$$C_{HTiO3} C_{BaOH} = C_{HTiO3,\infty} C_{BaOH,\infty} \exp(l/R_c) = K_{sp} \exp(l/R_c) \quad (6)$$

where equilibrium constant $K_{sp} = C_{HTiO3,\infty} C_{BaOH,\infty}$ for reaction 1 and is also called a solubility product, a function of temperature T when bulk $BaTiO_3$ is employed as the standard state and the effect of pressure is neglected. Equation 6 indicates that the value of R_c depends on the concentrations C_{BaOH} and C_{HTiO3} or, more exactly, on the product $C_{BaOH}C_{HTiO3}$. During coarsening, the C_{BaOH} and C_{HTiO3} decrease

(28) Sun, W. *Acta Mater*. **2005**, *53*, 3329.
(29) Lencka, M. M.; Riman, R. F. *Chem. Mater*. **1993**, *5*, 61.

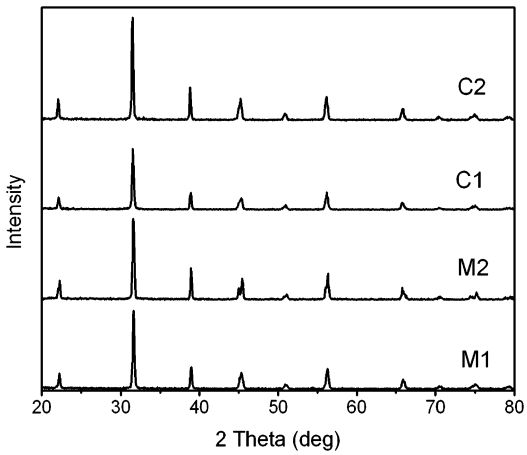

Figure 1. XRD patterns of $BaTiO_3$, where C1 and C2 are the CH samples synthesized at 220 °C for 14 and 168 h and M1 and M2 are the MH samples synthesized at 240 °C for 3 and 20 h, respectively.

monotonously with the growth of particles and hence R_c increases correspondingly.

Now, the attention is focused on the system in which the starting $Ba(OH)_2$/Ti molar ratio is larger than a unit. In this case, the basicity of the solution is maintained by the excess $Ba(OH)_2$, which keeps the pH >13. According to the thermodynamics data,[29] K_{sp} at temperatures below 240 °C is less than 1×10^{-14} mol^2/dm^6 so that C_{BaOH} and C_{OH} (the concentration of OH^-) can be treated as constants, approximately. Using C_{Ba} to denote the total concentration of the dissolved barium species, there is

$$C_{BaOH} = C_{Ba}\frac{C_{OH}}{C_{OH} + K_1} \tag{7}$$

where K_1 is the equilibrium constant for reaction $BaOH^+ = Ba^{2+} + OH^-$. Similarly, using C_{Ti} to denote the total concentration of the soluble titanium species and K_2 as the equilibrium constant for reaction $HTiO_3^- + 2H_2O = Ti(OH)_4 + OH^-$, the C_{HTiO3} is approximately expressed as

$$C_{HTiO3} = C_{Ti}\frac{C_{OH}}{C_{OH} + K_2} \tag{8}$$

Substituting eqs 7 and 8 into eq 6 and then differentiating it with respect to time t, we obtain

$$\frac{dC_{Ti}}{dt} = -K_{sp}\frac{(C_{OH} + K_1)(C_{OH} + K_2)}{C_{OH}{}^2 C_{Ba}}\frac{l}{R_c{}^2}\exp\left(\frac{l}{R_c}\right)\frac{dR_c}{dt} \tag{9}$$

The law of mass conservation in a closed system requires that the loss of Ti species in liquid phase must be equal to that gained in the solid phase, at any time, which can be expressed as

$$-V_{sln}\frac{dC_{Ti}}{dt} = \frac{1}{\upsilon_m}\int_0^\infty 4\pi R^2\left(\frac{dR}{dt}\right)f(R,t)dR \tag{10}$$

where $f(R,t)$ is the particle size distribution function and V_{sln} is the volume of the solution. The size change rate dR/dt can be expressed, via eq 4, as $dR/dt = \upsilon_m r_G = \upsilon_m k_g(C_{HTiO3}C_{BaOH} - C^*_{HTiO3}C^*_{BaOH})$. Recalling eqs 3, 5, and 6, and taking $\exp[(l/R) - (l/R_c)] \approx 1 + (l/R - l/R_c)$,[20] we get

$$\frac{dR}{dt} = k_{d,\infty}\upsilon_m l\left(\frac{1}{R_c} - \frac{1}{R}\right)\exp\left(\frac{l}{R_c}\right) \tag{11}$$

Therefore, by substituting eqs 9 and 11 into eq 10, we obtained

$$\frac{dR_c}{dt} = \frac{4\pi}{V_{sln}}\frac{k_{d,\infty}}{K_{sp}}\frac{C_{Ba}C_{OH}^2}{(C_{OH} + K_1)(C_{OH} + K_2)}R_c^3 n(t)\left(\frac{\overline{R^2}}{R_c^2} - \frac{\bar{R}}{R_c}\right) \tag{12}$$

where $\overline{R^2}$ and $\bar{R}$ are the averages of R^2 and R, i.e., $\overline{R^n} = (1)/(n(t))\int_0^\infty R^n f(R,t)dR$ and $n(t)$ is the number of particles at time t. The $n(t)$ is related to V_s, the total volume of the particles, by $n(t) = 3V_s/4\pi\overline{R^3}$ where $\overline{R^3}$ is the average of R^3. So, eq 12 transforms to

$$\frac{dR_c}{dt} = 3\Phi\frac{k_{d,\infty}}{K_{sp}}\frac{C_{Ba}C_{OH}^2}{(C_{OH} + K_1)(C_{OH} + K_2)}\frac{M_2 - M_1}{M_3} \tag{13}$$

where $\Phi = V_s/V_{sln}$ and $M_n = \overline{R^n}/R_c^n$ with $n = 1$, 2, and 3. The V_s and V_{sln} can be treated as being constants because of the very light supersaturation. According to LSW, there is $R_c \approx \bar{R}$.[20,30] Thus, $M_2 - M_1 = \overline{R^2}/R_c^2 - \bar{R}/R_c \approx (\overline{R^2} - \bar{R}^2)/R_c^2 = \sigma^2/R_c^2 > 0$, where σ^2 is the variance. In the space of reduced size $\xi = R/R_c$, $f(R,t)$ is transformed to $\varphi(\xi,t)$, i.e., $f(R,t)dR = \varphi(\xi,t)d\xi$. It has been theoretically proved that, as a zeroth approximation, $\varphi(\xi,t) = n(t)p(\xi)$, i.e., the scaled normalized distribution function $p(\xi)$ is time-independent,[20,30−32] whereas particle number $n(t)$ varies with time. Thus, the M_1, M_2, and M_3 values are independent of time, approximately.[28]

The solution to eq 13 is

$$\bar{R} = Kt + R_0 \tag{14}$$

where R_0 is the extrapolated radius at $t = 0$ and the rate constant K is

$$K = 3\Phi\frac{k_{d,\infty}}{K_{sp}}C_{Ba}\frac{C_{OH}{}^2}{(C_{OH} + K_1)(C_{OH} + K_2)}\frac{M_2 - M_1}{M_3} \tag{15}$$

Equation 14 predicts a linear growth law for $BaTiO_3$ particles during the early coarsening stage, as predicted for the unimolecular deposition reaction.[28]

IV. Results and Discussion

Particle Size and Morphology. Samples C1, C2, M1, and M2 are employed as representatives here. The C1 and C2 are the CH $BaTiO_3$ synthesized at 220 °C for 14 and 168 h, respectively, whereas samples M1 and M2 are the MH $BaTiO_3$ synthesized at 240 °C for 3 and 20 h, respectively. In Figure 1, the XRD patterns show that the samples are

(30) Slezov, V. V.; Sagalovich, V. V. *Sov. Phys. Usp.* **1987**, *30*, 23.
(31) Madras, G.; McCoy, B. J. *J. Colloid Interface Sci.* **2003**, *261*, 423.
(32) Mullins, W. W. *J. Appl. Phys.* **1986**, *59*, 1341.

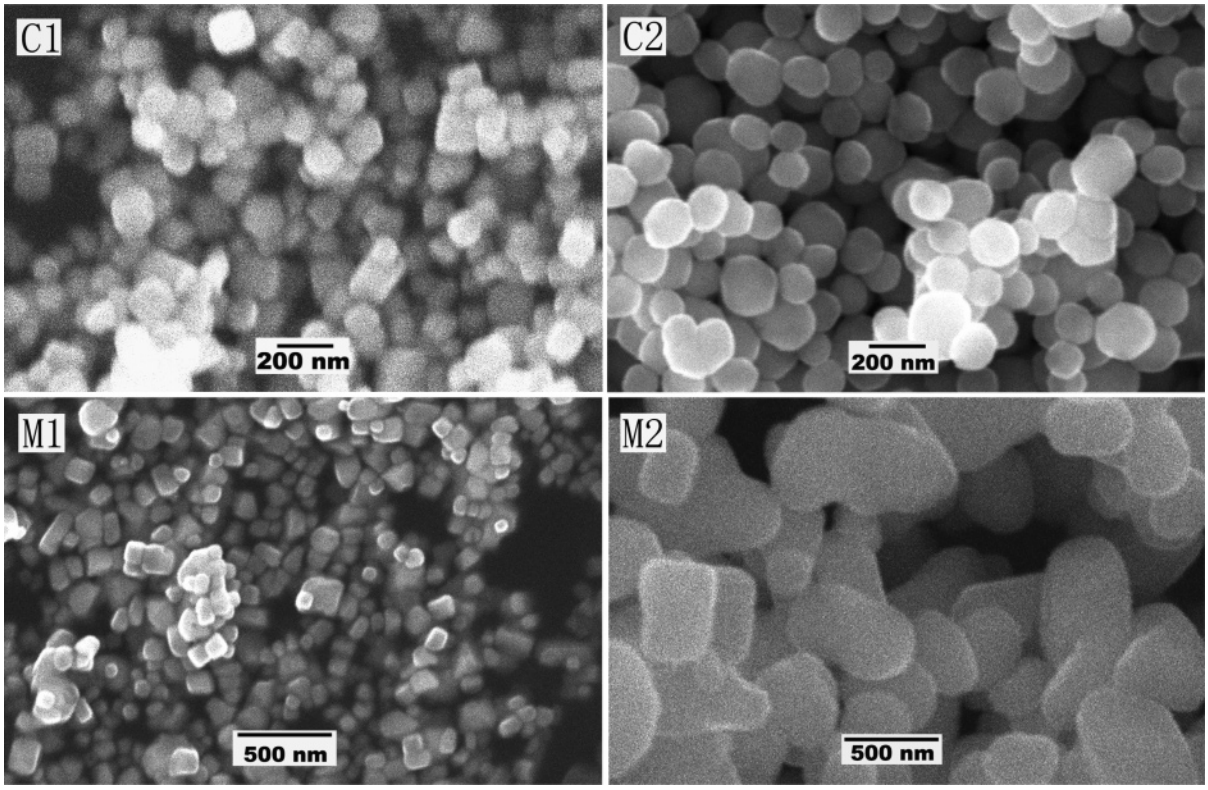

Figure 2. SEM photographs of $BaTiO_3$, where C1 and C2 are the CH samples synthesized at 220 °C for 14 and 168 h and M1 and M2 are the MH samples synthesized at 240 °C for 3 and 20 h, respectively.

crystalline and single-phase. No residual TiO_2 is detected. It was reported that the crystallization of TiO_2 was completed within 2 h in the CH process and 0.5 h in the MH process.[12] Thus, the particle growth of C1 to the C2, or the growth of M1 to the M2, originates from coarsening. Figure 2 shows the SEM photographs of these samples. The average size of sample C1 is 95 nm. When the reaction time is prolonged to 168 h, the size increases to 155 nm, determined from the micrograph of C2. The small particles observed in C1 are found to disappear in sample C2, which consists of uniform and bigger particles. This is an indication that particles grow through the coarsening mechanism. In contrast, the average sizes of M1 and M2 are 90 and 410 nm, respectively, but the time interval is only 17 h. This reveals that particle growth becomes much faster in a microwave field. We have noticed that the shape of the MH particles changes from cubic to round after prolonged treatment, which may cause a variation in the specific surface energy of the particles. However, we also observed that the change in shape is rather slow in comparison with the rapid particle growth, which means that there might be $|d\ln(\gamma/\gamma_0)/dt| \ll d\ln(R_c/R_0)/dt$ if using γ_0 to denote the initial specific surface energy of particles of the initial average radius R_0. In this case, eq 9 still holds, approximately. In eq 15, finally, the surface energy has no contribution to the rate constant K. It seems that the influences of the possible variation in surface energy due to the change in particle shape can be neglected approximately. In the sample M2, a few biparticles are observed. It suggests that particle coalescence or oriented attachment crystalline growth[33] may take place, to some degree, in the microwave field. The particle coalescence always leads to irregular particle shapes.[33] To estimate the contributions of the possible particle coalescence, the particle sizes measured from SEM (d_{SEM}) have been compared with the crystallite sizes d_{XRD} for the whole hydrothermal samples. Figure 3 shows that the relative deviations $(d_{XRD} - d_{SEM})/d_{SEM}$ are less than 25%, which indicates that most of the particles are single crystals. It seems that particle coalescence has little influence in the present work.

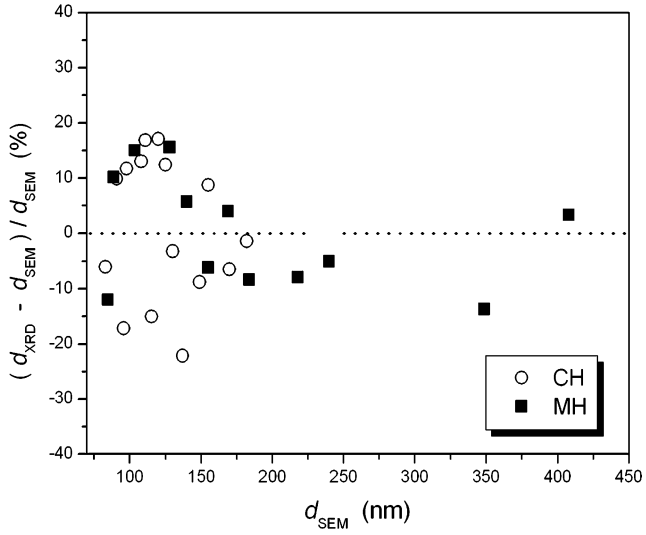

Figure 3. Comparison of the particle size measured from SEM (d_{SEM}) with the crystallite size estimated from XRD data (d_{XRD}).

Particle Growth. For all the samples synthesized, the average particle sizes were in the range of 85−410 nm. For agreement with eq 14, the particle "radius" R is used, which is half of the particle size. In Figure 4, the average radii of

(33) Huang, F.; Zhang, H.; Jillian, F.; Banfield, J. F. *J. Phys. Chem. B* **2003**, *107*, 10470.

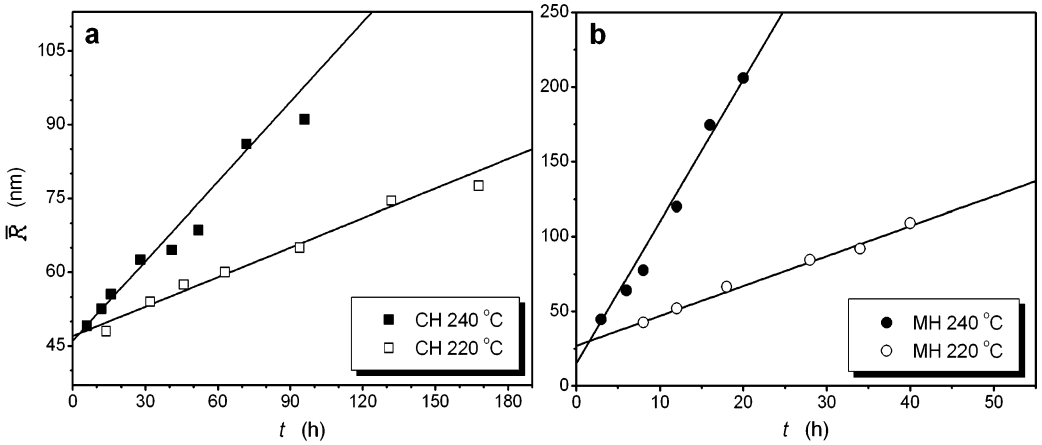

Figure 4. Average radii of (A) CH $BaTiO_3$ and (B) MH $BaTiO_3$ synthesized at 220 and 240 °C are plotted against aging time. The experimental data are well-fitted with linear lines. The volume fraction ($\sim V_s/V_{sln}$) of the coarsening phase $BaTiO_3$ is ~0.02 for all the samples.

CH and MH $BaTiO_3$ are plotted against reaction time. It shows that particles grow linearly with time for both CH and MH powders, as predicted by eq 14. The values of K and R_0 obtained by fitting the experimental data are listed in Table 1. Form the experimental K, kinetic coefficients k_g and $k_{d,\infty}$ can be estimated, which is concerned with the parameters in eq 15.

The volume fraction Φ of the coarsening phase is about 0.02 and the C_{Ba} is estimated to be ~1 mol/dm,[3] taking account of the water density in the temperature range 220−240 °C. From the thermodynamic data,[29] the values of constants K_1, K_2, and K_{sp} are evaluated. The K_1 is 0.094 mol/dm^3 at 220 °C and 0.079 mol/dm^3 at 240 °C. The K_2 is estimated to be 2.5 mol/dm^3 at 220 °C and 0.88 mol/dm^3 at 240 °C. The values of K_{sp} are 2.5×10^{-15} and 8.6×10^{-15} mol^2/dm^6 at temperatures of 220 and 240 °C, respectively. Thus, the C_{OH} is ~1.1 mol/dm.[3]

In theory, the normalized particle size distribution (PSD) in the reduced scale space is assumed to be approximately time-independent. Figure 5 exhibits the experimental PSDs with respect to scaled size $\xi = R/\bar{R}$, which are indeed independent of time in approximation. However, they are not consistent with the pattern predicted by LS[20] or that suggested by Hillter.[22] The measured PSDs are narrower than those predicted by the Hillert model and show a different asymmetry in comparison to the LS distributions. The LS or Hillert distribution is applicable to the coarsening system, controlled by diffusion or interface reaction, at sufficiently long times, whereas the coarsening system treated in this study is in the early stage. Through these PSDs, the experimental values of term $(M_2 - M_1)/M_3$ are measured by using $\bar{R}$ instead of R_c, as shown in Figure 6. The average values of $(M_2 - M_1)/M_3$ are 0.032 and 0.065 for the MH $BaTiO_3$ synthesized at 220 and 240 °C, respectively, and 0.044 and 0.057 for the CH $BaTiO_3$ synthesized at 220 °C and 240 °C, respectively. The deviations from the average value are small for each set of $(M_2 - M_1)/M_3$. However, a trend of decreasing $(M_2 - M_1)/M_3$ with time is observed. We have also noticed that the coarsening system at lower temperature has smaller $(M_2 - M_1)/M_3$, which will lead to slower particle growth according to eq 15.

Therefore, the values of $k_{d,\infty}$ and $k_g = k_{d,\infty}/K_{sp}$ are evaluated, which are summarized in Table 1. It shows that $k_{d,\infty}$ and k_g in the MH treatment are 1 order of magnitude larger than those in the CH one. From the values of $k_{d,\infty}$ or k_g at temperatures of 220 and 240 °C, estimation of activation energies is made, which gives close values for the CH and MH processes in both cases of $k_{d,\infty}$ and k_g. According to the collision theory, it is suggested that the much faster kinetics in the MH process might mainly arise from an increasing frequency of collision between reactant molecules due to the microwave irradiation According to reaction 1, it will cause both k_g and $k_{d,\infty}$ to increase. However, as only two reaction temperatures are employed here, this argument needs further examination. In the literature, it has been reported that the kinetics is enhanced by 1−2 orders of magnitude in the MH process,[34] which agrees with our observations. We are also aware that a number of materials can be quickly dissolved by the assistance of microwave irradiation.[35−36] In this model, greater k_d and k_g values in the MH process imply a faster dissolution of the small particles, whereas there is a quicker growth of the large particles.

Controlling Step. There were several reports that particle growth under hydrothermal conditions followed the third power law so that these coarsening processes were assumed to be diffusion controlled.[19,33,37−38] We are aware that the difference between the linear and the parabolic or even the cubic growth laws may be ambiguous if the investigation time is insufficiently long. In another previous work, we dealt with the competition between the two kinetic steps of diffusion and interface reaction, which occur in series.[39] It was shown that coarsening is diffusion-controlled when the diffusion coefficient D of solute satisfies to the condition $D/R_c \ll k_g$. If $D/R_c \gg k_g$, coarsening is controlled by the interface reaction. In this study, however, there are two solutes, $HTiO_3^-$ and $BaOH^+$, involved in the interface reaction. Because the $BaOH^+$ is in a large excess, its concentration can be regarded as being a constant during coarsening and hence the bimolecular reaction can be treated

(34) Komarneni, S.; Pidugu, R.; Li, Q. H.; Roy, R. *J. Mater. Res.* **1995**, *10*, 1687.
(35) Fischer, L. B. *Anal. Chem.* **1986**, *58*, 261.
(36) Kingston, H. M.; Jessie, L. B. *Anal. Chem.* **1986**, *58*, 2534.
(37) Huang, F.; Zhang, H.; Banfield, J. F. *Nano Lett.* **2003**, *3*, 373.
(38) Wong, E. M.; Bonevich, J. E.; Searson, P. C. *J. Phys. Chem. B* **1998**, *102*, 7770.
(39) Sun, W. *Acta Mater.* **2007**, *55*, 313.

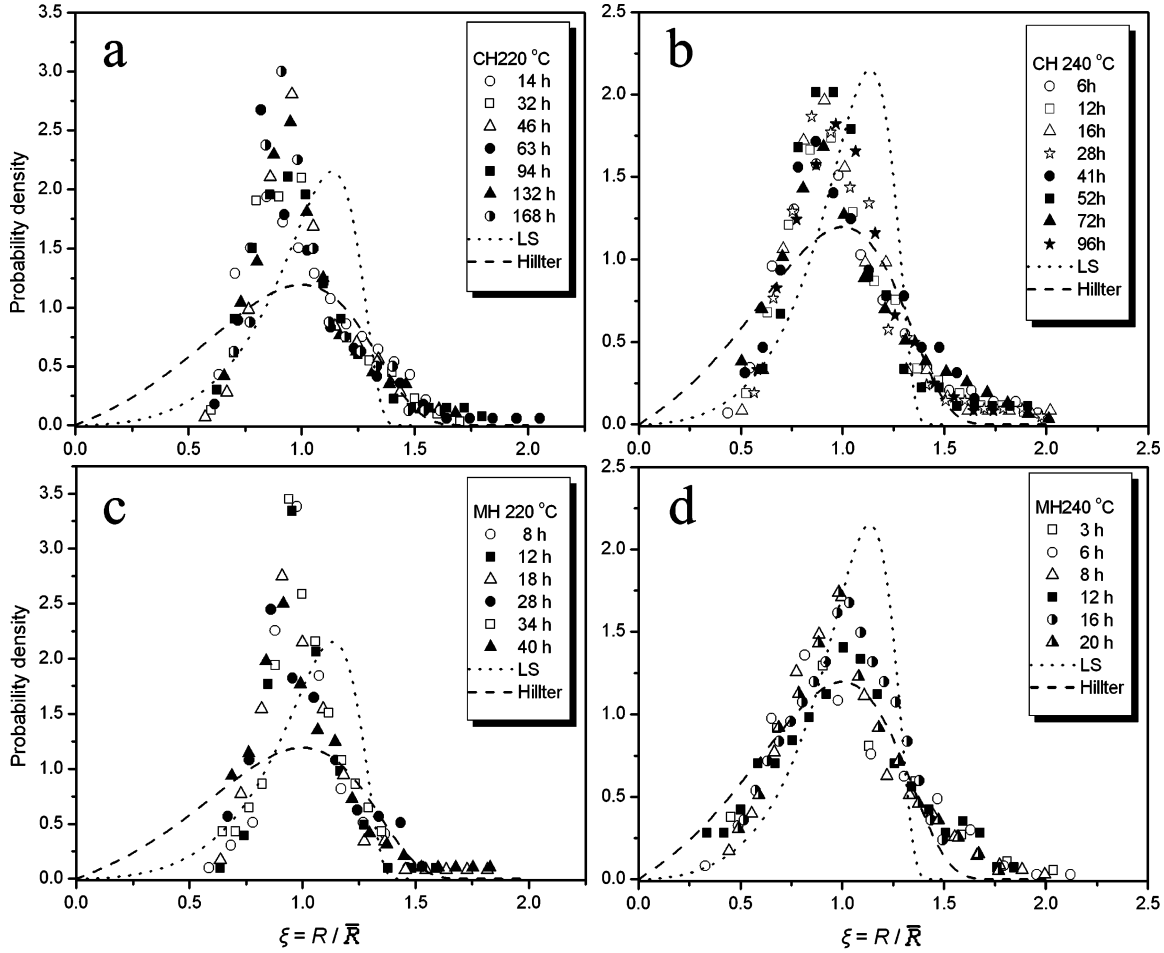

Figure 5. Particle size distributions with respect to reduced size $\xi = R/\bar{R}$ of $BaTiO_3$ synthesized by (a) the CH method at 220 °C, (b) the CH method at 240 °C, (c) the MH method at 220 °C, and (d) the MH method at 240 °C with different synthesis times noted in the panels.

Table 1. Kinetics Parameters for Coarsening of Hydrothermal $BaTiO_3$

method	T (°C)	K (nm/h)	R_0 (nm)	k_g ($m^4\ mol^{-1}\ s^{-1}$)	$k_{d,\infty}$ (mol $m^{-2}\ s^{-1}$)
MH	240	9.5	15	1.3×10^{-12}	1.1×10^{-20}
MH	220	2.0	27	1.0×10^{-12}	2.5×10^{-21}
CH	240	0.54	46	8.6×10^{-14}	7.4×10^{-22}
CH	220	0.20	47	7.6×10^{-14}	1.8×10^{-22}

as a pseudo-monomolecular reaction. Thus, by taking $C_{BaOH} \approx C_{Ba}$ and $R_c \approx \bar{R}$, the criteria become $D/\bar{R} \ll k'_g = k_g C_{Ba}$ for diffusion-controlled coarsening and $D/\bar{R} \gg k'_g$ for interface-controlled coarsening, where D denotes the diffusion coefficient of $HTiO_3^-$.

The largest value of k_g listed in Table 1 is less than 1×10^{-11} $m^4/(mol\ s)$ and C_{Ba} is ~1000 mol/m^3, so that k'_g is less than 1×10^{-8} m/s. Testino et al. estimated that the diffusion coefficient of $Ti(OH)_4$ at 80−90 °C is about 3×10^{-9} m^2/s.[19] By the Stocks−Einstein law, the value of D at 220−240 °C is estimated to be in the range 5×10^{-9} to 1×10^{-7} m^2/s, assuming the radius of $HTiO_3^-$ to be in the range 0.3−5 Å. Thus, even if taking $D = 1 \times 10^{-9}$ m^2/s and $\bar{R} = 1000$ nm, there is still $D/\bar{R} = 1 \times 10^{-3}$ m/s $\gg k'_g$. It indicates that the coarsening of hydrothermal $BaTiO_3$ in the present work ought to be controlled by the interface reaction.

Another indication is provided by the comparison between the values of $(\bar{R}^3_{i+1} - \bar{R}^3_i)/(t_{i+1} - t_i)$ and the rate constant $K_{(3)} = 8\nu_m^2\gamma DC_\infty/9R_AT$ for the third power law in the LSW theory.[20] $\bar{R}^3_i$ is the cube of $\bar{R}$ at the i-th time t_i. The molar volume ν_m of $BaTiO_3$ is 3.9×10^{-5} m^3/mol, and $C_\infty = K_{sp}/C_{BaOH}$ for solute $HTiO_3^-$ is 8.6×10^{-12} mol/m^3 at 240 °C and 2.4×10^{-12} mol/m^3 at 220 °C. The surface energy γ of $BaTiO_3$ in water is ~0.2 J/m^2.[19] Therefore, if D takes the larger value of 1×10^{-7} m^2/s, the $K_{(3)}$ is calculated to be $\sim 5 \times 10^{-32}$ m^3/s at 240 °C and $\sim 2 \times 10^{-32}$ m^3/s at 220 °C. In contrast, the smallest value of $(\bar{R}^3_{i+1} - \bar{R}^3_i)/(t_{i+1} - t_i)$, in

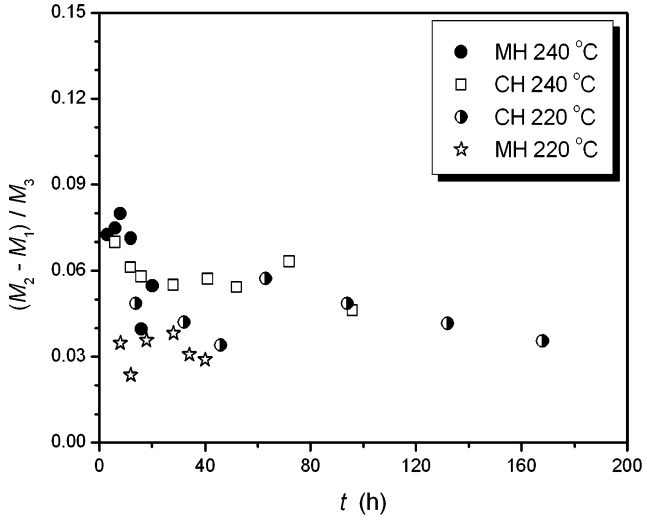

Figure 6. Values of $(M_2 - M_1)/M_3$ at different aging times for the CH and MH $BaTiO_3$ synthesized at 220 and 240 °C.

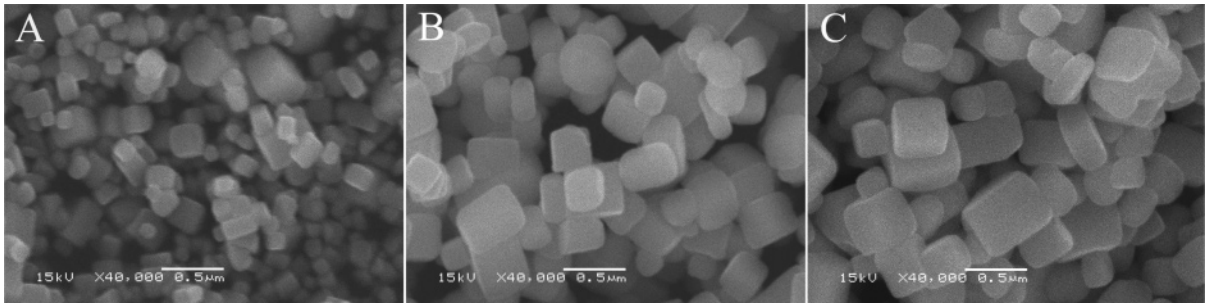

Figure 7. SEM images of CH $BaTiO_3$ synthesized at 240 °C with reaction times of (A) 140 h, (B) 264 h, and (C) 428 h.

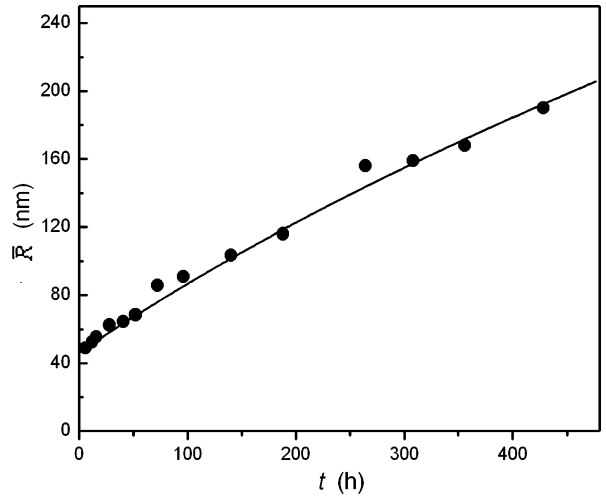

Figure 8. Average radii at different reaction times for CH $BaTiO_3$ synthesized at 240 °C are fitted with a curve calculated through eq 16.

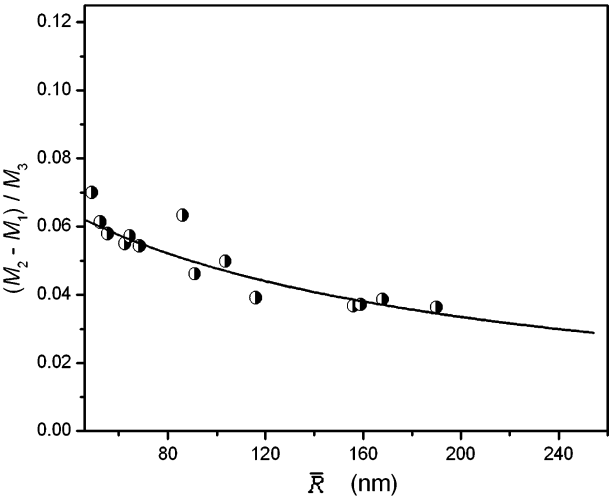

Figure 9. Values of $(M_2 - M_1)/M_3$ at different average radii of CH $BaTiO_3$ synthesized at 240 °C are fitted with a curve calculated through eq 17.

the case of CH $BaTiO_3$ synthesized at 220 °C, is 4×10^{-28} m^3/s, which is 4 orders of magnitude larger than the calculated values of $K_{(3)}$. The result suggests the third power growth law might not applicable for the present experiment.

Variation of Growth Exponent. The variation in the growth exponent in a coarsening process has been reported by several authors.[25,26,28,39,40] In the previous paper, we proposed that the linear growth in the early stage may transform to a parabolic growth if time is prolonged.[28] It was because the time-independence of factor $(M_2 - M_1)/M_3$ is only a zeroth approximate; after a long time, the factor will ultimately become zero.[28,30,39] To observe the variation in the growth exponent, we prepared more samples of CH $BaTiO_3$ at 240 °C with longer reaction times. The MH method was not used, so that possible particle coalescence could be avoided. Figure 7 exhibits the SEM images of CH $BaTiO_3$ synthesized at 240 °C for 140, 264, and 428 h. It clearly shows that particles become larger and more uniform when time is prolonged. The particles have a regular cubic shape. The average radii of CH $BaTiO_3$ particles synthesized from 6 to 428 h are plotted against reaction time in Figure 8. Apparently, eq 14 does not fit the experimental data over the full time scale. A second-order polynomial has been found to fit the data reasonably. Its expression is

$$t = \frac{\bar{R} - R_0}{K_{\mathrm{CH},1}} + \frac{\bar{R}^2 - {R_0}^2}{K_{\mathrm{CH},2}} \tag{16}$$

where a constant $K_{\mathrm{CH},1}$ of 0.54 nm/h and R_0 value of 46 nm are adopted from Table 1, and $K_{\mathrm{CH},2} = 222$ nm^2/h. Equation 16 gives a pattern for the transition of particle growth law from linear to parabolic. In Figure 9, the corresponding $(M_2 - M_1)/M_3$ values are given, plotted against $\bar{R}$. An empirical equation is found to describe the relationship between $(M_2 - M_1)/M_3$ and$\bar{R}$, which is

$$\frac{M_2 - M_1}{M_3} = \frac{a}{1 + b(\bar{R} - R_0)} \tag{17}$$

where $a = 0.062$, $b = 0.0055$ nm^{-1}, and $R_0 = 46$ nm. If formula 17 is substituted into eq 13, eq 16 can be deduced. Because $(M_2 - M_1)/M_3$ is determined by the particle size distribution, eq 17 suggests a slow evolution of the normalized PSD in the early stage, which appears to be the main cause for the variation in growth exponent. Formula 17 is an empirical expression obtained experimentally; however, considering that we should find $(M_2 - M_1)/M_3 \rightarrow 0$ when $t \rightarrow \infty$ (i.e., $R_c \rightarrow \infty$), it seems a reasonable approximation of $(M_2 - M_1)/M_3$ in the transition stage.

Effect of OH^-. It is generally accepted that in a strongly alkaline solution, the growth of hydrothermal $BaTiO_3$ is enhanced.[11,41] The explanation from the thermodynamic viewpoint is usually that $BaTiO_3$ is stable under basic conditions. However, Hertl has found that the growth rate of $BaTiO_3$ becomes independent of $Ba(OH)_2$ at concentrations greater than 1 mol/dm^3.[42] These behaviors can be

(40) Gösele, U.; Tu, K. N. *J. Appl. Phys.* **1982**, *53*, 3252.
(41) Flaschen, S. S. *J. Am. Chem. Soc.* **1955**, *77*, 6194.
(42) Hertl, W. *J. Am. Ceram. Soc.* **1988**, *71*, 879.

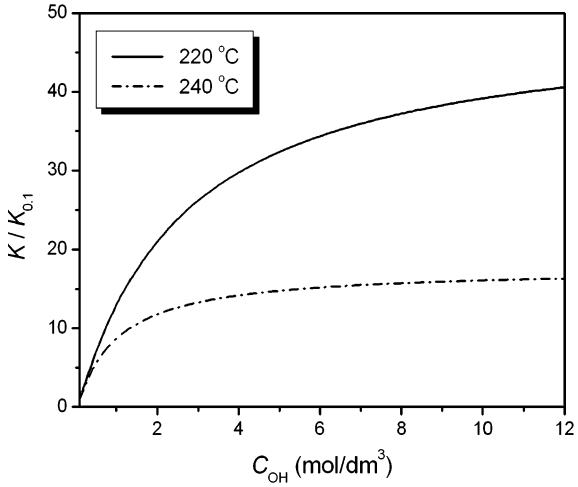

Figure 10. Ratios of rate constant K to $K_{0.1}$ at different base concentrations C_{OH}, where $K_{0.1}$ is the value of K at $C_{OH} = 0.1$ mol/dm^3.

understood through eq 15. In Figure 10, the ratio of rate constant K to $K_{0.1}$, the rate constant at $C_{OH} = 0.1$ mol/dm^3 is plotted versus C_{OH}. It shows an increase in K with increasing C_{OH}, indicating a promotional effect of OH^- on the growth of $BaTiO_3$. This effect is larger at low C_{OH} but becomes less important at high C_{OH} because of the slower increase in K. The effect of OH^- also exhibits a dependence on reaction temperature. Figure 10 shows that K at the lower temperature of 220 °C is more sensitive to the hydroxyl concentration.

V. Conclusions

Hydrothermal $BaTiO_3$ particles grow linearly with time in the early stage of coarsening controlled by a reversible interface reaction. At longer reaction times, the linear growth law changes to a parabolic growth law. The kinetic coefficients $k_{d,\infty}$ and k_g for the MH process are 1 order of magnitude larger than those for the CH process, which leads to much faster growth of $BaTiO_3$ particles in the MH process. Hydroxyl concentration has an enhancement effect on the growth of $BaTiO_3$ particles, especially at a lower base concentration or at a lower reaction temperature.

Acknowledgment. This work is supported by National Science Foundation of China under Grant 50471108.

CM061741N